Geopersia ***8*** *(2), 2018, PP. 199-212* *DOI: 10.22059/GEOPE.2018.238310.648337*

Petrology, geochemistry, and petrogenesis of mafic dykes from the Kermanshah Ophiolite in Sahneh-Harsin area of Western Iran

Farhad Aliani, Zeinab Daraeezadeh*
Department of Geology, faculty of science, Bu -Ali Sina University, Hamedan, Iran
**Corresponding author, e-mail: zeinab.daraee@gmail.com*
(*received: 02/08/2017 ; accepted: 05/03/2018*)

Abstract

The Kermanshah ophiolite complex is a part of the Mediterranean–Zagros–Oman Tethyan ophiolites, located in the structural–tectonic zone of western Iran in the northern part of the Zagros main thrust. Doleritic sheeted dykes are well exposed within the ophiolite in the south of Sahneh. These dykes contain high MgO, Na_2O, low TiO_2 (<0.1 wt %), P_2O_5, and K_2O contents, and high FeO^t/MgO and LILE/HFSE ratios. The geochemical data show that the parent magma of these dykes was an initial melt, tholeiitic subalkaline in nature; with LIL elements-enriched signature. N-MORB-normalized multi-element plots indicate nearly flat patterns for HFSE and enrichment in LILE; patterns of incompatible trace elements demonstrate an island arc affinity for these dykes. The enrichment of the LILE in comparison with HFSE suggests the involvement of a crustal component driven by fluids along the subduction zone. Several geochemical parameters suggest that the dykes of Kermanshah Ophiolite exhibit transitional characteristics between mid-ocean ridge basalt and island-arc tholeiite. High LILE/HFSE ratio negate suggest a mid-ocean ridge setting for these dykes; it is, therefore, proposed that the dykes may have originated in a back-arc basin tectonic setting or supra-subduction zone.

Keywords*: Sheeted Dykes; Tholeiite; Back-Arc-basin; Island Arc; Kermanshah Ophiolite*

Introduction

The sheeted dyke unit is an important component of most ophiolite suites. It occupies a specific horizon in the crustal sequence, directly below the pillow basalts and above the isotropic gabbros (Penrose Conference, 1972; Coleman, 1977). The presence of sheeted dykes in ophiolite suites was taken as being indicative of their formation in a sea-floor spreading setting. Some ophiolites show petrologic and geochemical similarities with crust generated at mid-ocean ridges (MOR). These include the large, relatively intact Tethyan ophiolites, such as Troodos in Cyprus, Semail in Oman, and so on (Alt *et al*., 1998; Yumul, 1996).

Sheeted dykes yield important geochemical information about the origin and tectonic setting of the magmas responsible for ophiolite formation. Firstly, their origin is directly related to major tectonic processes like sea-floor spreading. Secondly, sheeted dykes often serve as magma conduits between the underlying magma chamber and the overlying pillow basalts. The geochemistry of the sheeted dykes is often more reliable in determining the tectonic setting than that of gabbros and basalts from the same ophiolite suite (Pearce *et al.*, 1984; Nicolas, 1989; Leat *et al*., 2000; Rolland *et al*., 2000). The geochemistry of gabbros depends upon the relative proportion of cumulus minerals rather than the composition of the magma from which these rocks were crystallized. The basalts, particularly the pillow basalts, have often been subjected to reaction with seawater and hydrothermal alteration.

Although geochemical data on the Iranian ophiolites are relatively sparse, most of the available data suggests mid-ocean ridge basalt (MORB) and island arc tholeiite (IAT) affinities (Davodzadeh, 1972; Alavi-Tehrani, 1977; McCall & Kidd, 1981; Desmon & Beccaluva, 1983; Lippard *et al.,* 1986; Ghazi & Hassanipak, 1999; Allahyari *et al.,* 2010; Saccani *et al.,* 2013). Kermanshah Ophiolite (KO)—one of the fragmented Tethyan ophiolites (Broud, 1987; Shafaii Moghadam *et al.,* 2014; Shafaii Moghadam & Stern, 2011), widely considered to have formed in back-arc basin settings or the suprasubduction zone—is different from those formed at mid-ocean ridges (Allahyari *et al.,* 2010; Whitechurch *et al.,* 2013; Shafaii Moghadam *et al.,* 2014). Ophiolites of Iran have been assigned different modes of origin, whereas the KO is regarded as transitional between an island arc and an oceanic setting. Some geologists consider that the Eocene Kermanshah ophiolite in Kamyaran is an arc-related, suprasubduction zone ophiolite that formed in a back-arc extension setting based on its geochemical features (Vincent *et al.,* 2005; Whitechurch *et al.,* 2013; Ao *et al.,* 2015). According to Allahyari *et al.* (2010), the pegmatoid gabbros of KO show enriched-type mid-ocean ridge basalt (E-MORB)

chemistry, whereas the foliated gabbros have normal-type MORB (N-MORB) chemistry. The volcanic rocks of KO mainly consist of pillow basalts with subordinate massive lava flows; these volcanic rocks are represented by alkaline basalts and trachytes, as well as by sub-alkaline basalts with island arc affinity (Ghazi & Hassanipak, 1999).

This paper provides petrographic data and major and trace element geochemistry of sheeted dykes from the KO. The data presented in this paper will used to test the tectonic setting of this ophiolite.

Regional geology

Ophiolits of Iran, have been extensively examined in various aspects (e.g. Takin, 1972; Stocklin, 1974; Ricou, 1976; Berberian & King, 1981; Lippard *et al.,* 1986; Alavi, 1991; Arvin & Robinson, 1994; Hassanipak & Ghazi, 1996a; Shafahii Moghadam & Stern, 2011). Based on Shafahii Moghadam & Stern (2011) Mesozoic ophiolites of Iran are mostly Cretaceous in age, and are related to the Neotethys and associated back arc. These ophiolites can be subdivided into five belts: (1) Late Cretaceous Zagros outer belt ophiolites (ZOB) along the Main Zagros Thrust (2) Late Cretaceous Zagros inner belt ophiolites (ZIB) along the southern periphery of the Central Iranian block; (3) Late Cretaceous–Early Paleocene ophiolites of NE Iran; (4) Early to Late Cretaceous ophiolites in eastern Iran between the Lut and Afghan blocks; and (5) Late Jurassic–Cretaceous Makran ophiolites of SE Iran. ZOB ophiolites, which occur along the Zagros Suture Zone, extend from the Turkey-Iran border to just north of the Straits of Hormuz and constitute a significant part of the Alpine-Himalayan orogenic belt, containing numbers of important ophiolite complexes (Kermanshah, Neyriz ophiolites). These ophiolites and colored mélanges were formed as a result of the Neo-Tethys closure between Arabia and Eurasia along this suture zone.

The time of formation of the Zagros ophiolites and the closure of the Neo-Tethys Ocean are highly controversial. New zircon U–Pb age data show that the final closure of the Southern Neo–Tethys Ocean was in the Late Miocene–Early Pliocene (Ao *et al.,* 2015). Scarce radiometric data available for some diabases yielded ages ranging from 83 to 86 Ma (Delaloye & Desmons, 1980). The emplacement of the ophiolites occurred along the NE margin of the Arabian continent, marking the initial stage of collision that took place during the upper Cretaceous (Alavi, 1994).

The Zagros outer belt ophiolites are characterized by slices of sheeted dikes associated with pillowed and massive lavas (Shafahi moghadam & Robert, 2011). Zagros ophiolites are exposed in two separate sections: (1) Poshtkoh arc in Kermanshah (Braud, 1970), and (2) Fars arc in Neyriz (Ricou, 1971b). Neyriz and Kermanshah ophiolite complexes possess many compositional and constructional similarities with Oman radiolarite-ophiolite complex, Samail ophiolite, and ophiolites of the margin of Saudi Arabia (Aghanabati, 2007). The KO is located in the structural–tectonic zone of western Iran (Fig. 1) in the northern part of the Zagros main thrust and is a part of the highly dismembered Kermanshah–Panjvin ophiolite belt. The Zagros suture zone is situated between the Iranian Plate to the east and the Arabian block to the west. The Zagros collision zone in the NW of Iran comprises the internal Sanandaj–Sirjan, Gaveh Rud, and ophiolite zones, and the external Bisotun, Radiolarite, and High Zagros zones (Sadeghi & Yassaghi, 2016).

Local geology

The study area lies in the Zagros suture zone (Fig. 1) and can be divided into three main blocks: (1) radiolarite; (2) Kermanshah ophiolite, and (3) Bisotun limestone thrust sheets. The KO is strongly dismembered and comprises all segments of an ideal ophiolite suite (Fig. 2). Outcrops of KO, from north to south, are: (1) North East of Kermanshah (the Sahneh area) is composed of ultrabasic rocks with cumulate texture, peridotite, mostly harzburgite and pyroxenite, which are successively followed by gabbroic rocks, diabasic dykes, pillow lava, and intermediate–acidic volcanic rocks; ongoing with layered gabbros and dunite, which were less affected by extensive tectonics. (2) Southeast of this collection, in the Argana region, ultrabasic rocks are associated with the calcareous and radiolarian tiny intercalations. (3) In Harsin, a serpentinite body, there are pillow lava outcrops in which recrystallized bioclastic limestone (probably Miocene in age), are visible. (4) The serpentinized peridotites including dunite, harzburgite, and lherzolite, are exposed along the Harsin to Noorabad road and capped by Oligo–Miocene limestone, pillow lava, spilitic basalt, and isotropic gabbros. There are several bodies in the vicinity of Noorabad, mostly made up of isotropic gabbros. (5) In Gamassiab pass (Garin Mount.), various units are

mixed together as a result of tectonic forces and strongly dismembered, resembling a typical mélange.

This sequence is generally composed of ultramafic rocks at the base, followed upward by isotropic and layered gabbros and pillow basalts capped by pelagic sediments. The pelagic sediments occur as isolated bodies, intercalated with—and overlying—the pillow basalts. This section is devoid of plagiogranite. Almost all the lithotypes of this ophiolitic sequence are affected by static, ocean-floor metamorphism (peridotites, gabbroic sequences, dyke complex, and pillow lava), and regional metamorphism (peridotites and gabbros).

The KO is Late Cretaceous in age, and is thrusted over the Maastrichtian, which indicate post-Maastrichtian, and most probably Paleocene, emplacement of the ophiolite. A sequence of Eocene and the Olig–Miocene clastic-sedimentary rocks, Bisotun carbonates, and radiolarian chert formations unconformably overly the ophiolite, indicating Paleocene age for the emplacement of the ophiolite.

Field and petrographic relations

The KO contains various types of rocks occurring as dismembered fragments (Fig. 2). This sequence includes: (1) peridotites, ultramafics with tectonite texture, and those having cumulate texture; (2) gabbroic sequences; (3) a dyke complex; and (4) pillow lava. Peridotites are volumetrically the most abundant ophiolitic variety rocks (Saccani *et al*., 2013), represented by lherzolites, harzburgites, and dunites, locally intruded by pyroxenite dykes. The gabbroic sequence is represented by pegmatoid gabbros, amphibole gabbros, foliated and milonitic gabbros, and isotropic gabbros associated with troctolites and wehrlites.

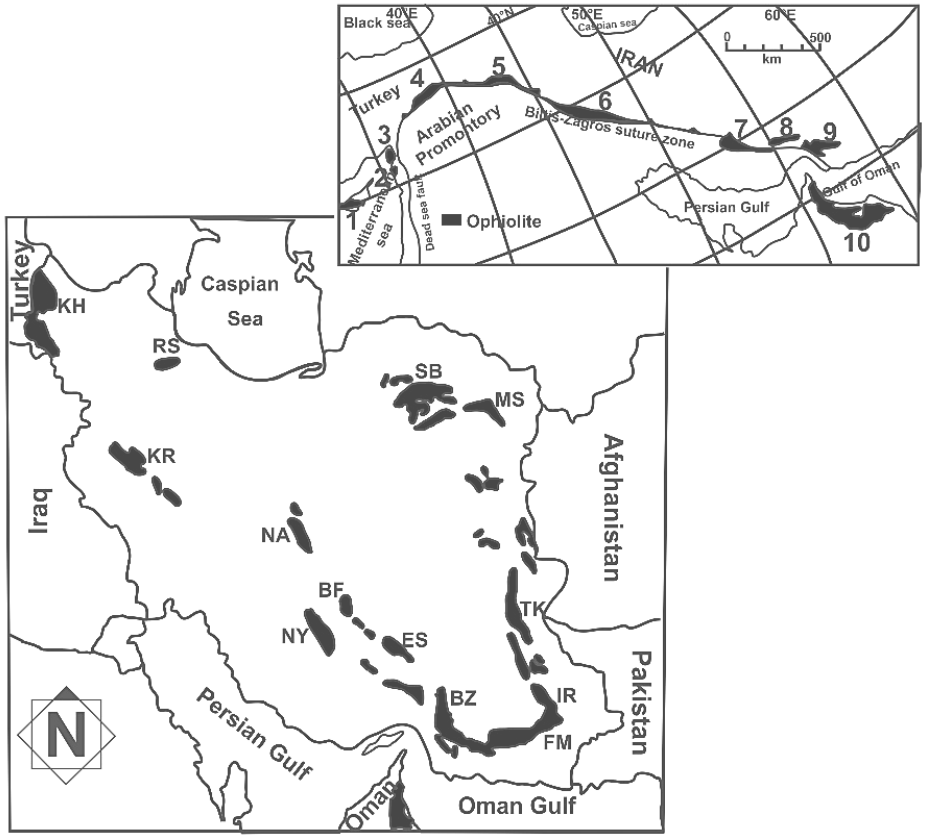

Figure 1. (a). Distribution of Cretaceous-Neo-Tethyan ophiolites around Arabian promontory (modifed after Dilek & Delaloy, 1992). 1. Troodos (Cyprus), 2. Baer-Bassit (Syria), 3. Kizildag (Turkey), 4. Guleman (Turkey), 5. Cilo (Turkey), 6. Kermanshah (Iran), 7. Neyriz (Iran), 8. Esphandagheh (Iran), 9. Band Ziarat (Iran), 10. Samail (Oman). (b) Enlarged area shows sketch map of Iran showing locations of major ophiolites. KH: Khoy, KR: Kermanshah, NY: Neyriz, BZ: Band Ziarat, NA: Naien, BF: Baft, ES: Esphandagheh, FM: Fanuj-Maskutan, IR: Iranshahr, TK: Tchehel Kureh, MS: Mashhad, SB: Sabzevar, RS: Rasht (Talesh ophiolite).

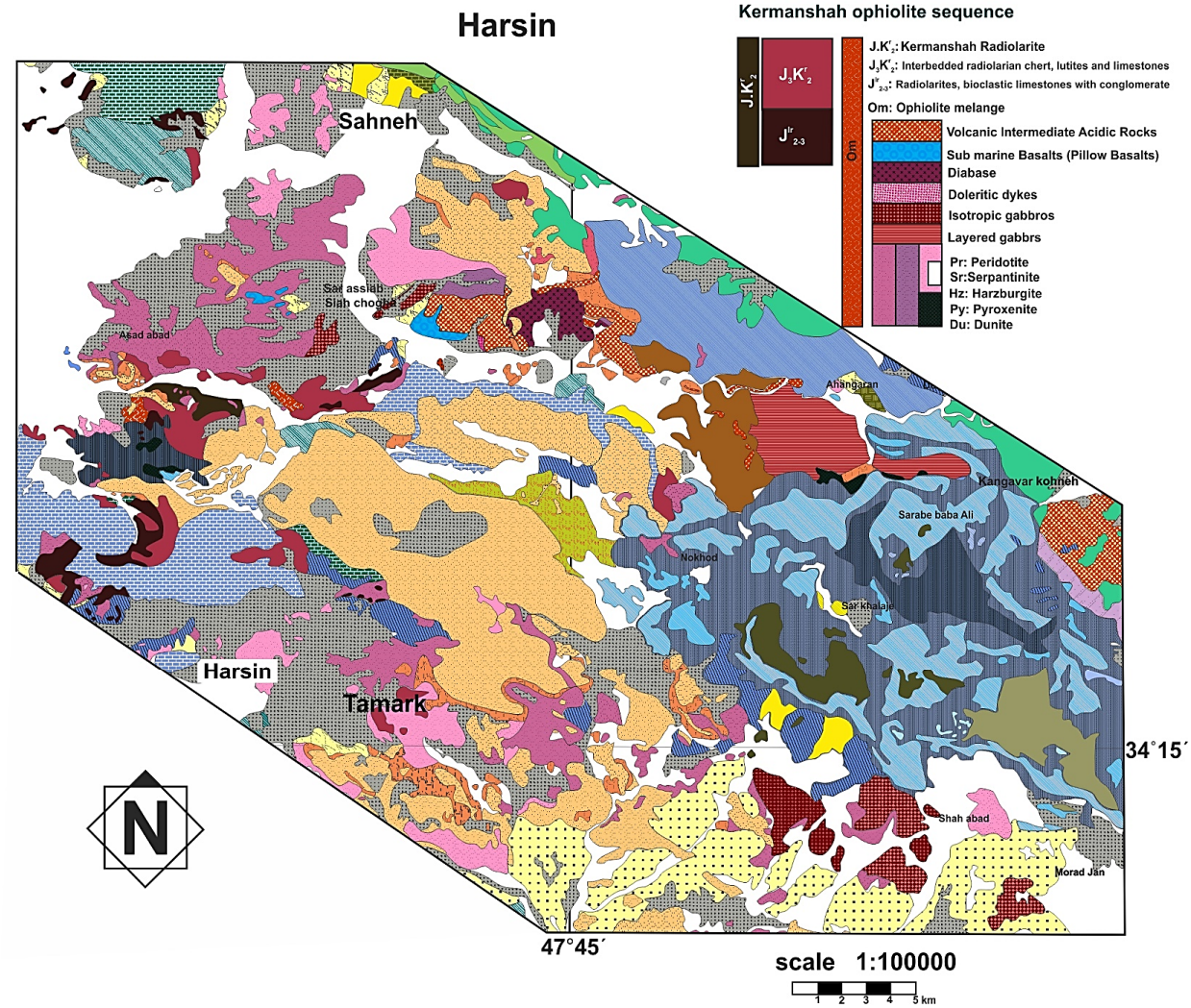

Figure 2. Geological map of the Kermanshah Ophiolite, SW Iran, modifed from the geological map of Harsin, Series 1:100,000 (Shahidi & Nazari, 1997).

A well-preserved volcanic sequence (including andesites, basaltic and pillow lava) and sheeted dyke complex are found in many places (e.g. south of Sahneh, east of Harsin and around Noorabad) that are intruded into basaltic lavas and covered by the Bakhtiari Formation (Pliocene) (Saccani *et al*., 2013).

The Kermanshah Ophiolite contains dyke swarms as well as isolated dykes (Fig. 3). Both types display sharp intrusive contacts with the basaltic rocks and are characterized by chilled margins. The sheeted dykes trend N-S, usually with a high dip angle. They range from a few centimeters to around five meters in width and may extend laterally for hundreds of meters. The sheeted dyke unit is well-exposed in the basal part of the south of Sahneh, in Ali-Abad village, where they intrude into basalts. Isolated dykes are sporadically distributed, irregularly oriented, and intrude all the ophiolitic rock types. These dykes crosscut, and so are younger than the sheeted dykes. Since no outcrop of lower basalt was observed in this region, hence, spilitic pillow lavas are absent. As they are extremely tectonized, it is impossible to draw a clear regional sequence between them. The dyke complex is also found in a few small outcrops along the Gamassiab river valley and around Tamrak village (across the Noorabad–Harsin Road).

The sheeted dykes are melanocrat, fine- to medium-grained, ophitic to subophitic and doleritic (Fig. 4). They are composed of plagioclase, clinopyroxene, hornblende, and magnetite (Fig. 4). Plagioclase (45-60% modal) occurs as laths in pyroxene and hornblende and as inclusions within

poikilitic diopsidic–augite poikocrysts. The plagioclase is partly to completely altered to sericite, calcite, and epidote. Quartz grains, developed after the decomposition of plagioclase, are identified in most dyke samples.

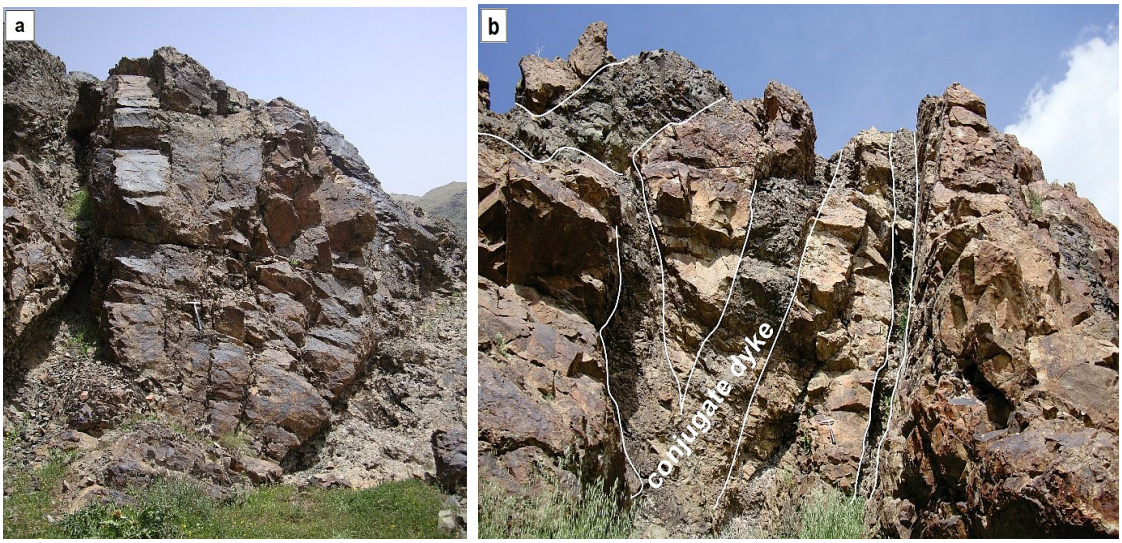

Figure 3. Outcrops of diabasic dykes near the Ali abad village, view to the southeast.

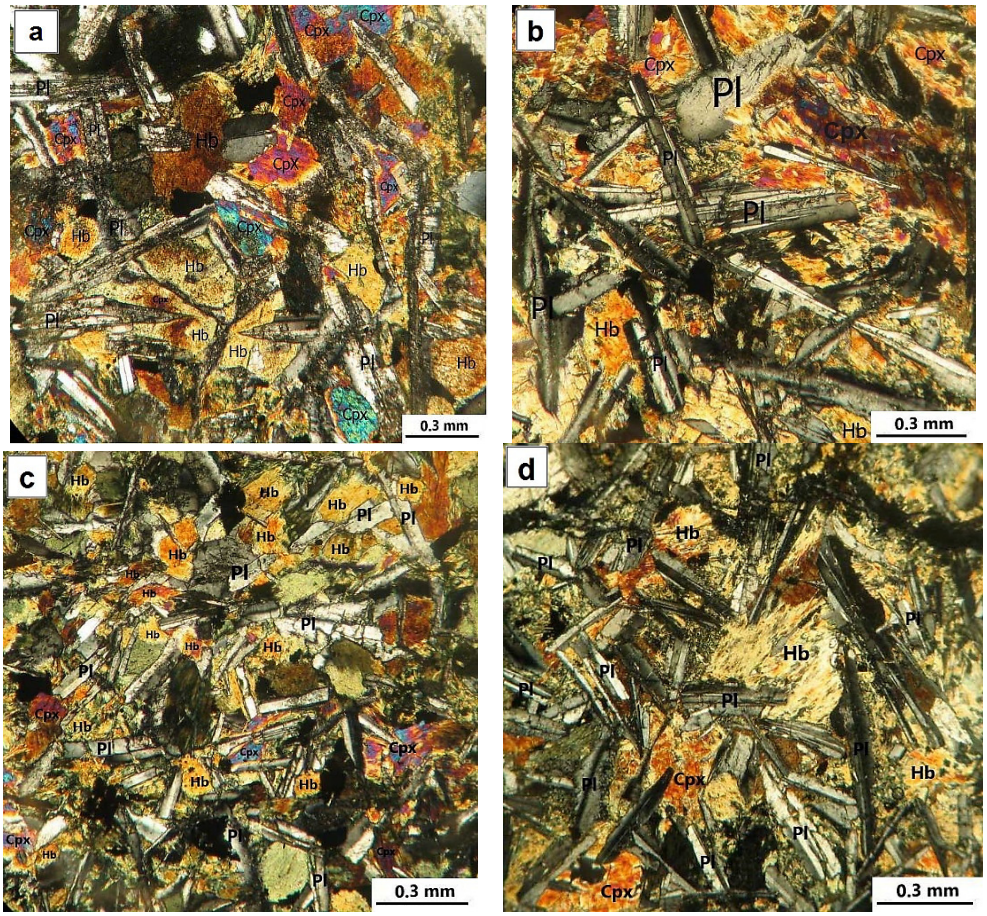

Figure 4. Photomicrographs of diabasic dykes (Photos were taken under XPL). Ophitic to subophitic texture in sheeted dykes of Kermanshah ophiolite. Abbreviations: Ol: olivine; Opx: orthopyroxene; Cpx: clinopyroxene; Plg: plagioclase; Hb, hronblende.

Clinopyroxenes are the most important mafic mineral of this rock unit and show very distinct zoning. The clinopyroxenes are diopsidic–augite (locally augite), making 10–15% modal of the dykes, and is altered, partly to completely, to amphibole and magnetite. Its primary texture, however, is preserved (Fig 4c, d).

Amphibole forms up to 15% modal and can be divided into two generations. Primary (igneous) amphibole is brownish and pleochroic. In contrast, the secondary amphibole is bluish-green and ranges from equant grains to slender (uralitic) fibers. The former (primary) is normally common hornblende and the secondary amphibole is actinolite and/or tremolite. The hornblende (reaching up to 20% modal) is commonly altered to chlorite, but replaced by biotite in some places. Modal percentages of this mineral are not identical in all sections. The lighter dykes have a greater amount of plagioclase than darker ones.

Opaque minerals include magnetite, hematite, and ilmenite, which are present in almost all the dykes up to 5% modal frequency. Skeletal and anhedral magnetite grains, identified within and around the clinopyroxene grains, appear to be formed from the decomposition of clinopyroxene. The secondary mineral assemblage (calcite, epidote, chlorite, amphibole, and secondary quartz and albite) suggests that the dykes have been subjected to metamorphism under greenschist facies conditions. Most of the rocks studied are also affected by post-magmatic processes like hydrothermal alteration and/or weathering.

Analytical methods

Eighteen samples of the sheeted dyke swarm from the KO were analysed in SGS laboratory in Canada. Whole-rock major and some trace element analyses were obtained using ICP-AES (ICP95A). Volatile contents were determined as loss on ignition at 1000 °C. In addition, Rb, Sr, Y, Zr, Nb, Hf, Ta, Th, and U, and rare earth elements (REE) were determined by inductively coupled plasma-mass spectrometry (ICP-MS) using an IMS95A, Lithium Metaborate fusion / ICP-MS finish. Representative analyses are presented in Table 1 correspond to rock samples that were less affected by alteration and postmagmatic processes such as hydrothermal alteration and/or weathering.

Geochemistry

The geochemical features of the diabasic dykes, belonging to KO in the Sahneh–Harsin area, are described using whole-rock major and some trace and rare earth elements, which are virtually immobile during low-temperature alteration and metamorphism.

Sheeted dykes are basaltic in composition, displaying a clear sub-alkaline nature, as exemplified by their low Nb/Y ratios (<0.16), which is shown in the Nb/Y versus Zr/TiO_2 * 0.0001 diagram (Fig. 5a).

They are soda (Na_2O)-rich, potash-deficient, and have high magnesium tholeiite (Middlemost, 1975, 1994; Miyashiro, 1975; Ross & Bédard, 2009; Figs. 5b-d). They are enriched in Fe_2O_3, FeO^t/MgO ratios and characterized by low TiO_2 (mostly <1.0 wt %) and P_2O_5 contents (Table 1, Figs. 6a and b). Based on correlation coefficients, the dykes show a fractionation trend when tested on Zr (ppm) versus MgO (wt.%), TiO_2 (wt.%), Y (ppm) variation diagrams (Figs. 7a-c), suggesting a co-magmatic origin for the dykes. The dataset of the dykes is plotted on the N-MORB normalized incompatible element patterns (Sun & Mc Donough, 1989) and chondrites normalized spider diagram (Boynton, 1984) (Figs. 8a, b).

These dykes thereby show almost similar and nearly flat geochemical patterns for HFSE with insignificant depletion in P, Zr, and enrichment in LILE, such as Ba, Rb, K, Th and Sr. This variation, with more enrichment of LIL compared to HFS elements, might be due to alteration and/or crustal contamination (Pearce *et al*., 1984; Yumul & Balce, 1994; Yumul, 1996).

However, it is noteworthy that a strong negative Nb anomaly, with reference to K and Sr, the characteristic property of the rocks found in the island-arc suite, was not observed. In chondrites normalized rare earth elements pattern (Thompson, 1982), all samples are about 10 times richer in REEs than chondrites despite the fact that in the majority of igneous arc basaltic magmas (IAB), there is selective enrichment of Rb, Ba, or K, compared with light earth elements, as expected (Wilson, 1996).

Alterations in low temperatures in mid-ocean basalts cause changes in various elements, especially mobile elements. Hence, Ba enrichment in ophiolite dykes of Sahneh-Harsin area is a good indicator of the degree of alteration (see Table 1 and Fig. 8).

Table 1. Representative major (wt.%) and trace element (ppm) concentrations for dykes from the Kermanshah ophiolite.

Sample. no	KO.D 1	KO.D 6	KO.D 7	KO.D 8	KO.D 10	KO.D 12	KO.D 15	KO.D 22	KO.D 24	KO.D 25	KO.D 26	KO.D 27	KO.D 28	KO.D 29	KO.D 30	KO.D 31	KO.D 32	KO.D 33
Major elements, wt %																		
SiO_2	48.1	49.1	47.2	47.3	48.3	47.9	48.4	47.7	48.4	44.3	48.2	49.3	47.2	47.1	49.7	44.1	45.3	48.5
Al_2O_3	14.5	15.1	15.7	15.1	15.2	14.5	13.9	14.5	14.1	15.1	15.4	14.3	15.9	16.3	13. 9	16.5	16.6	15.0
Fe_2O_3	10.7	12.3	11.3	10.9	10.2	11.7	11.1	9.85	12.4	8.87	11.8	11.2	11.2	10.7	8.69	8.94	11.4	10.0
MnO	0.21	0.21	0.22	0.22	0.17	0.21	0.24	0.21	0.26	0.18	0.22	0.21	0.20	0.29	0.14	0.17	0.22	0.21
MgO	7.98	7.39	7.78	7.78	8.44	7.26	7.66	8.58	6.85	7.26	7.58	7.56	8.51	8.71	10.1	8.57	7.89	8.60
CaO	10.64	9.86	11.3	11.4	10.7	8.99	11.4	11.5	10.5	12.9	10.58	9.77	11.4	12.3	12	10.06	11.6	12.0
Na_2O	2.75	2.8	2.0	2.3	2.5	3.7	2.6	2.2	2.6	2.5	2.4	3.2	1.9	1.7	1.8	2.46	2.1	2.3
K_2O	0.31	0.35	0.23	0.22	0.43	0.25	0.37	0.19	0.21	0.11	0.29	0.34	0.31	0.14	0.09	0.27	0.23	0.19
P_2O_5	0.07	0.09	0.07	0.08	0.06	0.10	0.07	0.06	0.09	0.08	0.08	0.07	0.08	0.08	0.04	0.07	0.06	0.06
Cr_2O_3	0.04	0.03	0.04	0.02	0.05	0.03	0.02	0.05	<0.01	0.03	0.03	0.02	0.03	0.03	0.13	0.04	0.03	0.03
TiO_2	1.11	1.41	1.07	0.93	0.96	1.42	1.14	0.93	1.36	0.59	1.24	1.16	0.77	0.78	0.72	0.82	0.98	0.86
Sum	98.4	100.9	98.8	98.6	99.3	98.9	98.1	97.3	98.1	96.7	99.85	99.5	99.2	99.5	99.1	95.6	98.1	99.2
LOI	2.0	2.15	1.75	2.3	2.27	2.92	1.32	1.50	1.28	4.70	1.95	2.36	1.73	1.40	1.68	3.68	1.75	1.43
Trace elements, ppm																		
Ba	120	150	100	110	130	140	140	80	50	60	130	100	200	150	50	210	100	80
Ce	5.45	6.3	5.0	7.6	5.2	6.8	5.7	4.1	7.7	6.2	5.7	7.4	9.0	7.4	7.1	5.1	5.0	4.5
Dy	4.52	4.59	3.63	3.48	4.06	4.54	4.54	3.75	5.40	1.99	4.11	4.57	2.64	2.59	3.13	2.99	3.77	3.68
Er	2.97	3.06	2.38	2.27	2.53	2.99	2.84	2.35	3.62	1.28	2.72	3.02	1.78	1.65	2.07	1.93	2.26	2.54
Eu	0.92	1.09	0.85	0.83	0.81	1.15	0.96	0.75	1.26	0.57	0.97	0.96	0.66	0.69	0.72	0.64	0.83	0.82
Gd	3.17	3.8	2.86	2.7	3.21	3.75	3.23	2.67	4.19	1.63	3.33	3.51	2.12	2.04	2.38	2.19	2.78	2.84
Hf	2	2	1	1	1	2	2	1	2	<1	1	2	<1	<1	2	1	1	1
Ho	0.89	0.94	0.76	0.74	0.86	0.98	0.96	0.76	1.17	0.45	0.85	0.99	0.56	0.53	0.63	0.62	0.78	0.81
La	2.2	2.3	1.7	3.5	2.3	3.0	2.2	1.5	2.9	3.2	1.9	3.2	4.7	3.9	3.1	2.4	1.8	2.2
Lu	0.35	0.39	0.30	0.36	0.33	0.36	0.38	0.30	0.62	0.17	0.35	0.40	0.21	0.21	0.27	0.27	0.31	0.34
Nb	2	2	2	2	2	2	2	2	2	2	2	2	2	2	1	2	1	2
Nd	5.7	6.8	5.3	6.2	5.3	7.1	5.9	4.6	8.2	4.6	6.1	7.2	5.7	5.2	5.4	5.5	5.3	4.9
Pr	0.97	1.1	0.87	1.13	0.95	1.2	0.98	0.74	1.38	0.83	0.98	1.24	1.18	1.01	1.05	0.8	0.89	0.79
Rb	1.8	2.9	1.6	1.7	2.7	1.8	1.7	1.1	0.9	0.9	2.2	3.2	2.5	1.4	1.3	2.9	1.7	1.2
Sm	2.2	2.5	2.0	1.9	2.0	2.6	2.4	1.9	2.9	1.2	2.3	2.4	1.6	1.5	1.8	2.0	2.0	1.9
Sr	140	270	170	160	120	180	170	110	120	100	230	130	230	240	120	200	160	110
Tb	0.59	0.65	0.55	0.58	0.55	0.66	0.64	0.51	0.83	0.30	0.6	0.64	0.37	0.37	0.43	0.42	0.50	0.53
Th	0.1	0.1	0.1	<0.1	0.1	0.1	0.1	<0.1	0.1	0.7	0.1	0.3	0.5	0.5	0.4	0.1	0.1	<0.1
Tm	0.38	0.43	0.34	0.32	0.36	0.40	0.41	0.34	0.51	0.18	0.38	0.44	0.24	0.23	0.3	0.28	0.34	0.35
U	0.05	0.06	0.10	0.16	<0.05	0.06	0.05	<0.05	0.07	0.22	0.8	0.14	0.19	0.19	0.14	0.05	0.10	0.05
V	271	336	316	281	247	346	259	222	283	235	320	266	296	304	257	186	302	232
Y	24.1	26.1	20.4	19.9	22.6	26.8	25.6	21.6	31.8	11.9	23.2	26.1	15.2	13.9	17.4	17.5	21.2	22.2
Yb	2.6	2.7	2.3	2.1	2.4	2.8	2.7	2.3	3.5	1.2	2.5	2.8	1.6	1.5	2	2.3	2.1	2.4
Zr	51.1	55.6	43.5	43.6	47.7	57.9	56.4	42.6	72.8	22.9	50	69.4	26.2	26.7	50.5	44.3	41.4	45.6

Tectonic setting of the dykes

In the TiO_2-P_2O_5*10-MnO*10 diagram (Mullen, 1983), the sheeted dykes infer an island arc tholeiite (IAT) field, excluding one sample, which falls on the Boninite field (Fig. 9a). The FeO_t–MgO–Al_2O_3 diagram (Pearce *et al.*, 1977) demonstrates that the dykes are located in the ocean floor basalts and island arcs fields (Fig. 9b). In the Zr/4-Nb*2-Y diagram (Meschede, 1986), all sample plots are in the volcanic arc basalt and N-MORB field (Fig. 9c). The La/10-Y/15-Nb/8 diagram of Cabanis & Lecolle (1989) shows most sample plots in the volcanic arc tholeiites, backarc basin basalts, and N-type MORB fields.

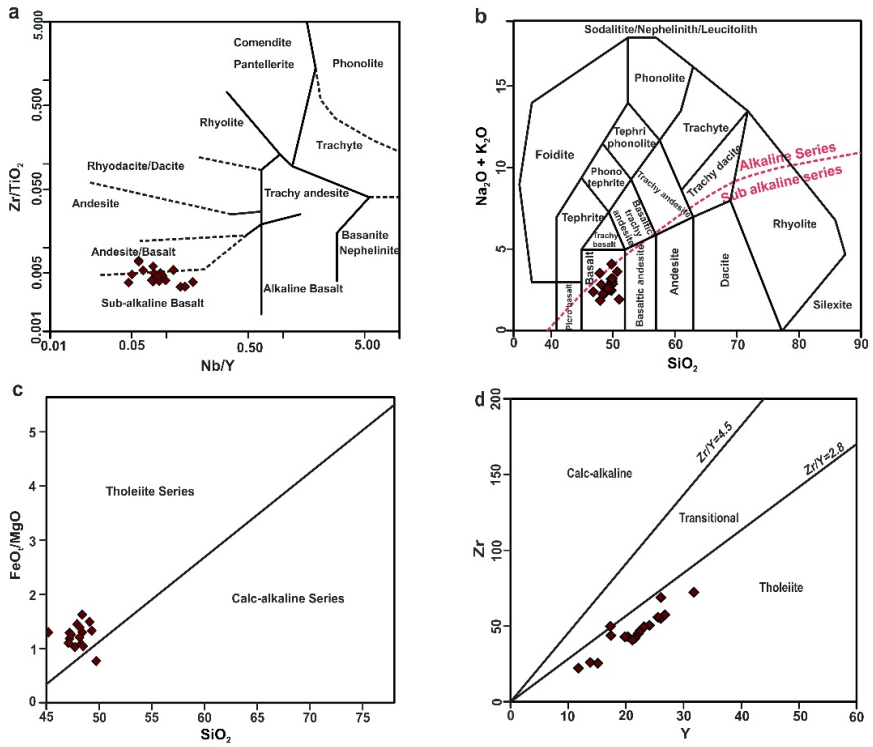

Figure 5. (a) $Zr/Ti0_2 \times 0.0001$ vs. Nb/Y diagram for classification of the Kermanshah dykes (fields are after Winchester & Floyd, 1977). (b) Chemical classification of igneous rocks that utilize total alkali vs. silica (TAS) (Middlemost, 1994); (c): FeO/MgO vs. SiO_2 diagram for classification of the Kermanshah dykes (after Miyashiro, 1975). (d) Zr (ppm) vs. Y (ppm) diagram from Ross & Bédard (2009), indicating that the protoliths of rocks had a tholeiitic basalt origin. Filled diamond: sheeted dykes.

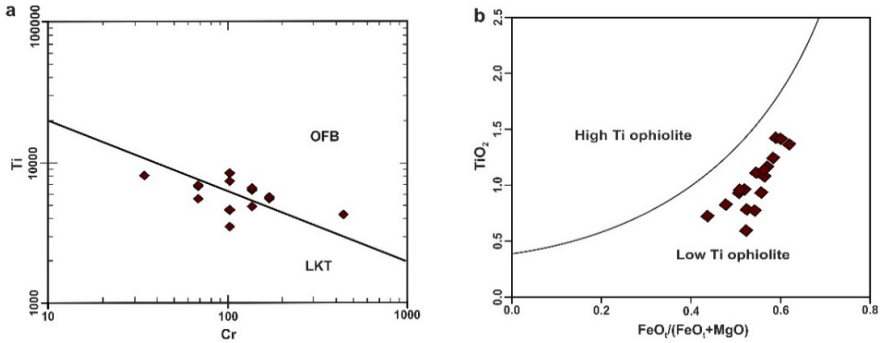

Figure 6. (a) Log Cr-Log Ti diagram (Pearce, 1975). (b) TiO_2-FeO*/FeO*+MgO) diagram (Serri, 1981) for samples of dykes. Filled diamond: sheeted dykes (the abbreviations used in the figure a include OFB: Oceanic Floor Basalts and LKT: Low K Tholeiite).

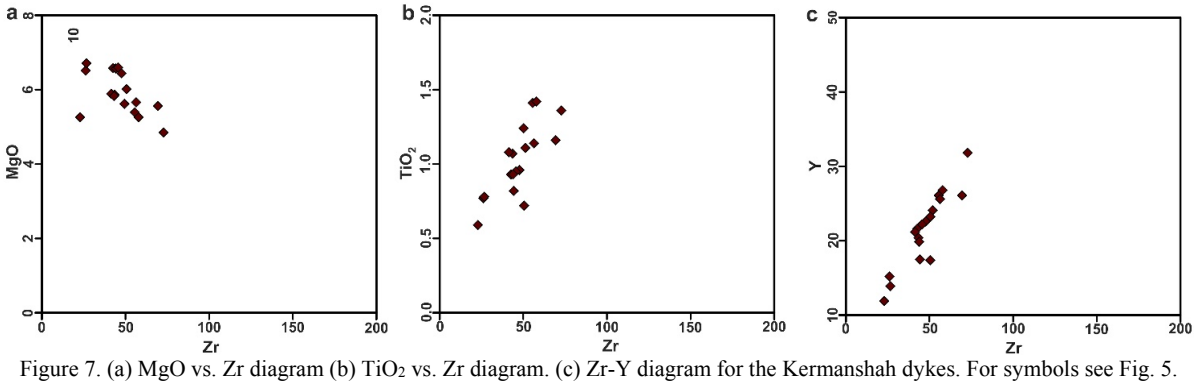

Figure 7. (a) MgO vs. Zr diagram (b) TiO_2 vs. Zr diagram. (c) Zr-Y diagram for the Kermanshah dykes. For symbols see Fig. 5.

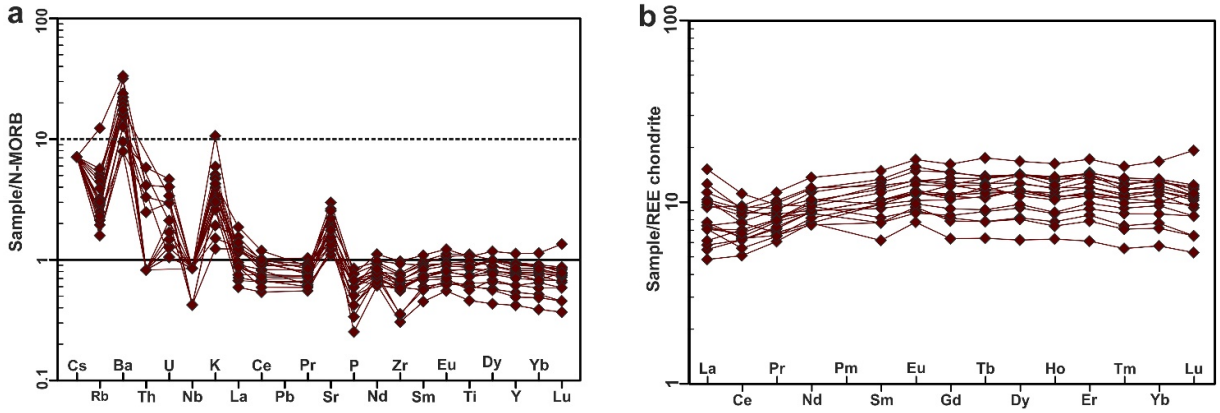

Figure 8. (a) N-MORB normalized incompatible element patterns, normalizing values are from Sun & McDonough (1989), and (b) Chondrite-normalized REE patterns, normalizing values are from Boynton (1984) for the dykes from the Kermanshah ophiolite complex.

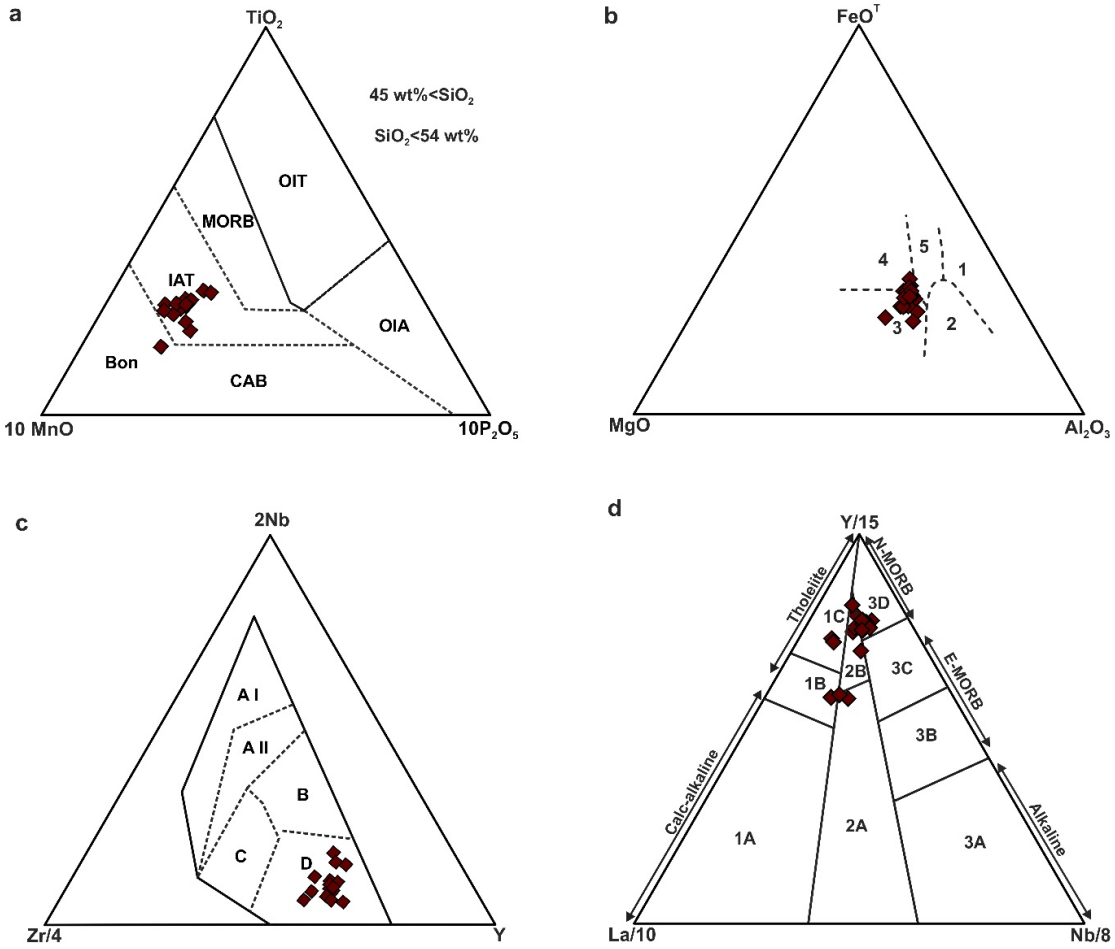

Figure 9. (a) MnO*10-TiO_2-P_2O_5*10 diagram (Mullen, 1983); (the abbreviations used in the figure include OIT: Oceanic Island Tholeiites; MORB: Mid-Ocean Ridge Basalt; OIB: Oceanic Island Basalt; IAT: Island Arc Tholeiite; CAB: Continental Arc Basalt; BON: Boninite); (b) MgO-FeO_t-Al_2O_3 diagram (Pearce et al., 1977); fields are: 1: Spreading center island; 2: Orogenic; 3: Oceanic ridge and Floor; 4: Oceanic island and 5: Continental; (c) Zr/4-Nb*2-Y diagram (Meschede, 1986), (fields are: A I: Within plate alkali basalts (WPA); A II: WPA/Within plate tholeiite (WPT); B: P-MORB; C: WPT/Volcanic arc basalts (VAB) and D: VAB/N-MORB); (d) La/10-Y/15-Nb/8 diagram (Cabanis & Lecolle, 1989) for the Kermanshah dykes; (fields are: 1A: Calc□alkaline basalts; 2A: continental basalts; 3A: alkali basalts from intercontinental rift; 1C: volcanic arc tholeiites; 1B: overlap between 1A and 1C; 2B: backarc basin basalts; 3B and 3C: E□type MORB; 3B: enriched; 3C: weakly enriched; 3D: N□type MORB). Symbols as in Fig. 5a.

The plot of Zr/Y versus Zr diagram (Pearce & Norry, 1979) shows that the dykes are transitional between two basaltic types. According to Shervais (1982), V and Ti play an important role in discriminating between basalts of various tectonic settings, with sheeted dykes from the Kermanshah ophiolite plot in a zone that characterizes island arc mid-oceanic ridge basalts (Fig. 10b). The results of the depiction of the data in Ti-Zr (Fig. 11a), Ti/100-Zr-Y*3 (Fig. 11b), and Ti/100-Zr-Sr/2 (Fig. 11c) diagrams (Pearce & Cann, 1973) suggest that the studied dykes belong to mid-ocean ridge basalts and island arc tholeiites (IAT).

On the basis of log-transformed functions of immobile trace element ratios, La/Th, Sm/Th, Yb/Th, and Nb/Th, Agrawal et al. (2008) recently constructed a new set of tectonic discrimination diagrams. These diagrams successfully distinguish between IAB (Island arc basalts), mid-ocean ridge basalts (MORB), ocean island basalts (OIB), and continental rift basalts (CRB). On the IAB-OIB-MORB-CRB diagrams, the rocks plot in the MORB-IAB fields (Fig.12). On the IAB-MORB-CRB-OIB diagram (Fig. 12a), they display a trend projecting from MORB to IAB field, with decreasing La/Th, Sm/Th, Yb/Th, and Nb/Th ratios (Fig. 12).

Discussion and conclusions

Sheeted dykes of the KO were originally basaltic in composition and seem to be co-magmatic (Fig. 5a). Good positive correlation between Zr with MgO, TiO_2, and Y prove minimal alteration effects and show that they form a single magmatic series (Fig. 7a, b and c). Moreover, variations in Zr and correlated elements may also reflect the fractional crystallization of mafic minerals.

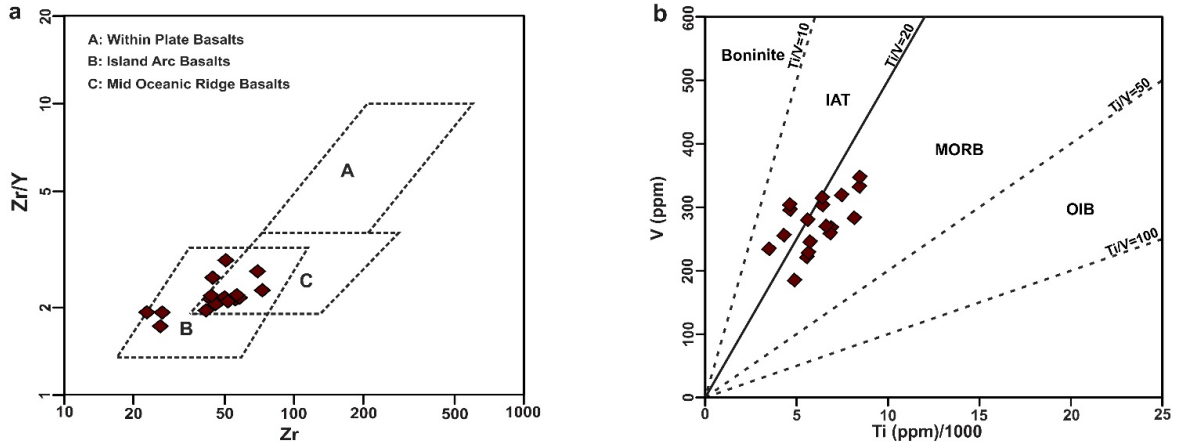

Figure 10. (a) Zr vs. Zr/Y diagram for the Kermanshah dykes (fields are after Pearce & Norry, 1979); A: Within plate basalt (WPB); B: Island-arc basalts (IAB); C: Mid-ocean ridge basalt (MORB); (b) Ti vs. V diagram for the dykes (fields are after Shervais, 1982); OIB: Oceanic island basalt; MORB: Mid-ocean ridge basalt; IAT: Island-arc tholeiite and Boninite. Symbols as in Fig. 5.

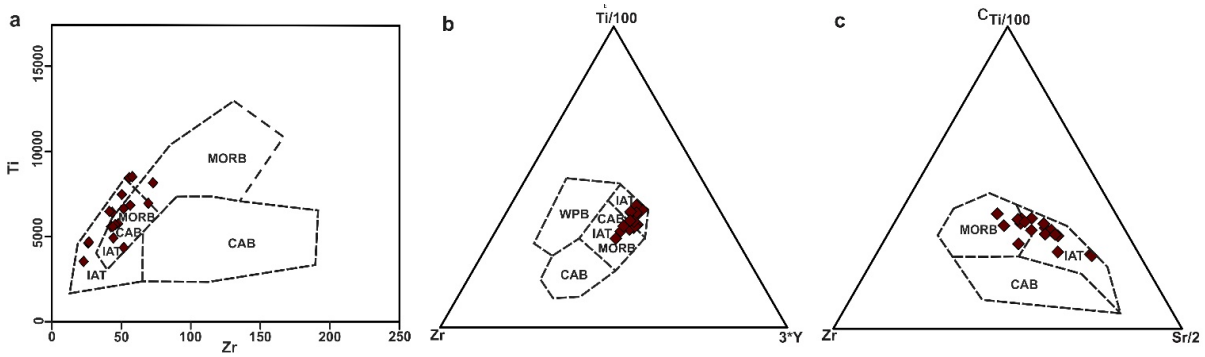

Figure 11. (a) Ti-Zr; (b) Zr-Ti/100-Y*3 and (c) Zr-Ti/100-Sr/2 determining tectonic setting diagrams (Pearce & Cann, 1973). The abbreviations include; MORB: Mid-Ocean ridge basalts; IAT: Island Arc tholeiites; CAB: Continental Arc Basalts; WPB: Within Plate Basalts. Symbols as in Fig. 5.

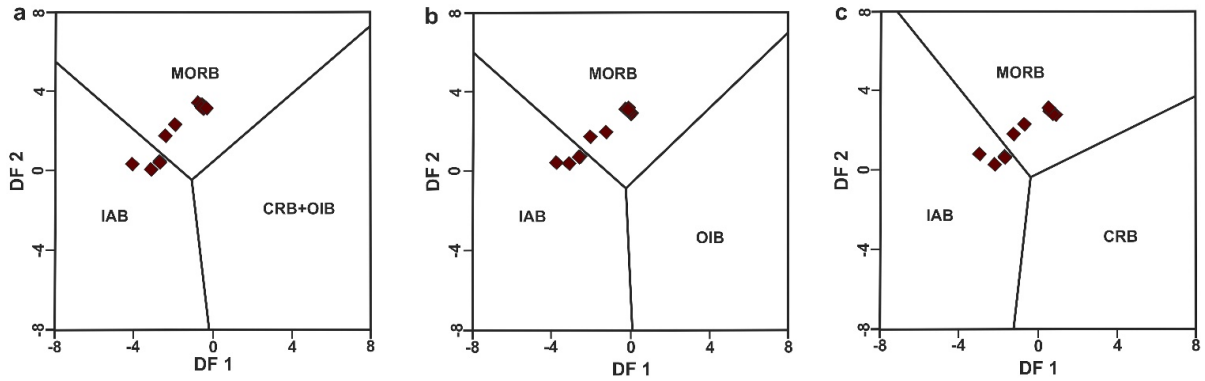

Figure 12. Logtransformed immobile trace element tectonic discrimination diagrams, suggesting that the Kermanshah ophiolitic sheeted dykes originated in an island arc tectonic setting (adopted from Agrawal *et al*., 2008). For diagram (a): DF1 = 0.3518 loge (*La*/*Th*) + 0.6013 loge (*Sm*/*Th*) – 1.3450 loge (*Yb*/*Th*) + 2.1056 loge (*Nb*/*Th*) – 5.4763; DF2 = –0.3050 loge (*La*/*Th*) – 1.1801 loge (*Sm*/*Th*) + 1.6189 loge (*Yb*/*Th*) + 1.2260 loge (*Nb*/*Th*) – 0.9944; (b): DF1 = 1.7517 loge (*Sm*/*Th*) – 1.9508 loge (*Yb*/*Th*) + 1.9573 loge (*Nb*/*Th*) – 5.0928; DF2 = –2.2412 loge (*Sm*/*Th*) + 2.2060 loge (*Yb*/*Th*) + 1.2481 loge (*Nb*/*Th*) – 0.8243; (c): DF1 = 0.3305 loge (*La*/*Th*) + 0.3484 loge (*Sm*/*Th*) – 0.9562 loge (*Yb*/*Th*) + 2.0777 loge (*Nb*/*Th*) – 4.5628; DF2 = –0.1928 loge (*La*/*Th*) – 1.1989 loge (*Sm*/*Th*) + 1.7531 loge (*Yb*/*Th*) + 0.6607 loge (*Nb*/*Th*) – 0.4384; MORB: Mid-Ocean Ridge Basalts; OIB: Ocean Island Basalts; IAB: Island Arc Basalts and CRB: Continental Rift Basalts.

Based on tectonomagmatic diagrams, the dykes show transitional characters between N-MORB and IAT; most dykes have island arc tholeiite (IAT) affinities that negate a typical mid-ocean ridge origin for these dykes. This raises the possibility that the dykes may have originated in a marginal basin.A fore-arc origin for the dykes cannot be advocated because of the absence of rocks typical of fore-arcs, particularly boninites, which are common in present-day active fore-arcs—for example, the Marianas Saunders & Tarney, 1984; Alt *et al*., 1998). N-MORB normalized multi-element patterns of the dykes show flat patterns for HFS-elements and enrichment of LILE (Ba, Rb, K, Th, Sr). The enrichment of the LILE in comparison with HFSE, with negative Nb anomalies in these dykes, suggest the involvement of crustal components, added to the overlying mantle by fluids rising along a subduction zone. REEs exhibit slightly depleted LREE patterns, geochemically similar to island arc tholeiites. Several geochemical parameters suggest that the dykes of Kermanshah Ophiolite exhibit transitional characteristics between mid-ocean ridge basalt and island-arc tholeiite. High LILE/HFSE ratio negates suggest a mid-ocean ridge setting for these dykes, and, so, it is proposed that these dykes may have originated in a back-arc basin tectonic setting.

On immobile trace element ratio tectonomagmatic discrimination diagrams (Fig. 12), the dykes from the Kermanshah ophiolite fall in the field of either MORB or MORB to island arc basalt, and display a trend projecting from MORB to IAB field, with decreasing La/Th, Sm/Th, Yb/Th, and Nb/Th ratios (Fig. 12). This trend is interpreted to reflect the enrichment of the depleted upper mantle by subduction-derived components following the initiation of intra-oceanic subduction and arc migration (Polat, 2011). According to Dilek & Furnes (2011), during subduction initiation, magma is generated, first of all, from decompression melting of fertile lherzolitic mantle, and forms the earliest crustal units with MORB-affinity characteristics. Island arc magma produced in a subarc-forearc melting column, which is subsequently emplaced. Accordingly, we suggest that the dykes of the KO may have formed in a back arc setting.

Based on field observation criteria, petrographic observations along with the inferred tectonic setting of the Zagros thrust and geochemical data presented here, the dykes of the KO are thus interpreted to have formed in a back-arc basin or supra-subduction zone. The composition of ophiolitic rocks formed in a back-arc basin setting are characterized by a higher concentration of large-ion lithophile elements (LILE), non-depletion of Nb, low-Ti content, and highly differentiated nature (from basalt to rhyolite), as compared to mid-ocean ridge basalts (Saunders & Tarney, 1979; Pearce *et al*., 1984; Harper *et al*., 1988; Schiffman & Fridleifsson, 1991; Jones et al., 1991; Bloomer et al, 1995; Yumul, 1993, 1996; Leat *et al*., 2000). The back-arc basin or supra-subduction zone setting for KO is supported by some chemical characteristics of the sheeted dykes include: (1) Transitional chemistry from MORB to island-arc

tholeiites; (2) the V-Ti relations; and (3) the enrichment of HFSE compared with island arc tholeiite and the depletion of HFSE, excluding Nb, compared with N-MORB.

Acknowledgement

The authors are grateful to Dr. H. Mohseni Faculty member of Geology department of Bu -Ali Sina University, Hamedan for their constructive reviews of this paper**.**

References

Aghanabati, S. A., 2007. Geology of Iran. A Publication of the Geological Survey of Iran, 586pp. (in Persian).

Alavi, M., 1991. Tectonic Map of the Middle East. Geological Survey of Iran.

Alavi-Tehrani, N., 1977. Geology and petrography in the ophiolitic range of Sabzevar (Khorassan/Iran) Geological Survey of Iran. Report 43.

Allahyari, K., Saccani, E., Pourmoafi, M., Beccaluva, L., Masoudi, F., 2010. Petrology of mantle peridotites and intrusive mafic rocks from the Kermanshah ophiolitic complex (Zagros belt, Iran): implications for the geodynamic evolution of the Neo-Tethyan oceanic branch between Arabia and Iran. Ofioliti, 35: 71–90.

Alt, J.C., Teagle, D.A., Brewer, T., Shanks, W.C., Halliday, A., 1998. Alteration and mineralization of an oceanic-fore-arc and the ophiolite ocean crust analogy. Journal of Geophysical Research, 103: 12365-12380.

Ao, S., Xiao, W., Khalatbari Jafari, M., Talebian, M., Chen, L., Wan, B., Ji, W., Zhang, Z., 2015. U–Pb zircon ages, field geology and geochemistry of the Kermanshah ophiolite (Iran): From continental rifting at 79 Ma to oceanic core complex at ca. 36 Ma in the southern Neo-Tethys. Gondwana Research, 31: 305-318.

Arvin, M., Robinson, P.T., 1994. The petrogenesis and tectonic setting of lavas from the Baft Ophiolitic Melange, southwest of Kerman, Iran. Canadian Journal of Earth Sciences, 31: 824-834.

Bloomer, S.H., Taylor, B., Macleod, C.J., Stern, R.J., Freyer, P., Hawkins, J.W., Johnson, L, 1995. Early arc volcanism and the Ophiolite problem: In a perspective from drilling in the western Pacific. In: Taylor, B., Natland, J. (Eds.). Active Margins and Marginal Basins of the Western Pacific. Geophysical Monograph Series, 188: 1-10.

Braud J., 1970. Les formation au Zagros dans la region de Kermanshah (Iran) et leurs rapports structuraux", Compt. Rend. Geological Survey of Iran, Report 271: 244-1291.

Braud, J., 1987. La suture du Zagros au niveau de Kermanshah (Kurdistan Iranien): Reconstitution paleogeographique, evolution geodynamique, magmatique et structurale [Ph.D thesies]: Universite Paris-Sud, 489p.

Boynton, W. V., 1984. Cosmochemistry of the earth elements: meteorite studies. In: Henderson, R. (Ed.), Rare Earth Element Geochemistry: Developments in Geochemistry, 2. Elsevier, Amsterdam: 89-92.

Cabanis B., Lecolle M., 1989. The La/10-Y/15-Nb/8 Diagram: A Tool for Discrimination Volcanic Series and Evidencing Continental Crust Magmatic Mixtures and/or Contamination. Compte Rendus de l'Academie des Sciences, Seris II, Mécanique, Physique, Chimie, Sciences de l'univers, Sciences de la Terre 309(20): 2023–2029 (in French).

Coleman, R.G., 1977. Ophiolites: Ancient Oceanic Lithosphere. Spinger-Verlag, New York, 229.

Davoudzadeh, M., 1972. Geology and petrography of the area north of Nain, Central Iran. Geological Survey of Iran, Report 39.

Delaloye, M., Desmons, J., 1980. Ophiolites and mélange terranes in Iran: a geochronological study and its paleotectonic implications. Tectonophysics, 68: 83–111.

Ghazi A.M., Hassanipak A, A., 1999. Geochemistry of subalkaline and alkaline extrusives from the Kermanshah ophiolite, Zagros Suture Zone, Western Iran: Implications for Tethyan plate tectonics. Asian Journal of Earth Sciences, 17: 319-332.

Desmons, J., Beccaluva, L., 1983. Mid-ocean ridge and island-arc affinities in ophiolites from Iran: palaeographic implications. Chemical Geology, 39: 39–63.

Dilek Y., Furnes, H., 2011. Ophiolite genesis and global tectonics: geochemical and tectonic fingerprinting of ancient oceanic lithosphere. Geological Society of America Bulletin, 123: 387–411.

Hassanipak A. A., Ghazi A. M., Wampler J. M., 1996a. REE characteristics and K/Ar ages of the Band Ziarat ophiolite complex, southeastern Iran", Canadian Journal of Earth Sciences, 33: 1534- 1542.

Harper, G.D., Bowman, J.R., Kuhans, R., 1988. A field, chemical and stable isotope study of subsea floor metamorphism of Josephine Ophiolite, California-Orogen. Journal of Geophysical Research, 93: 4625-4656.

Irvine T.N., Baragar W. R. A., 1971. A guide to the chemical classification of the common volcanic rocks. Canadian Journal of Earth Science, 8: 523-548.

Jensen L. S., 1976. A new cation plot for classifying subalkalic volcanic rocks", Ontario Division of Mines Mp 66 22.

Jones, G., Robertson, A.H.F., Cann, J.R., 1991. Genesis and emplacement of the supra-subduction zone Pindos Ophiolite, northwestern Greece. In: Letters, T.y., Nicolas, A., Coleman, R.G. (Eds.), Ophiolite Genesis and Evolution of the Oceanic Lithosphere: 771-799.

Leat, P.T., Livermdre, R.A., Millar, I.L, Pearce, J.A., 2000. Magma supply in back-arc spreading center segment E2, East

Scotia Ridge. Journal of Petrology, 41: 845-866.
Lippard S. J., Shelton A. W., Gass I. G., 1986. The ophiolite of Northern Oman., Geological Society of London Memoir 11, 178 p.
McCall, G.J.H., Kidd, R.G.W., 1981. The Makran, southeastern Iran: the anatomy of a convergent plate margin active from Cretaceous to present. In: Legget, J. (Ed.). Trench-fore arc geology, 10. Geological Society Special Publication (London): 387-397.
Meschede, M., 1986. A method of discriminating between different types of mid-ocean ridge basalts and continental tholeiites with the Nb-Zr-Y diagram. Chemical Geology, 56: 207-218.
Middlemost, E.A.K, 1975. The basalt clan. Earth Science Review, 11: 337-364.
Middlemost E. A. K., 1994. Naming materials in the magma/igneous rock system. Earth Sciences Review, 37: 215- 224.
Miyashiro, A., 1975. Volcanic rock series and tectonic setting. Earth and Planetary Science Letters, 3: 251-269.
Mullen, E. D., 1983. $MnO/TiO_2/P_2O_5$ a minor element discriminate for basaltic rocks of oceanic environment and its implication for petrogenesis. Earth and Planetary Science Letters, 62: 53-62.
Nicolas, A., 1989. Structure of ophiolites and dynamics of ocean lithosphere. In: Petrology and Structural Geology, 4. Kluwer Academic Publication, London, p. 365.
Pearce, J. A., 1975. Basalt geochemistry used to investigate past tectonic environment on Cyprus, Tecnophysics 25, 41-67.
Pearce, J. A., Cann, J. R., 1973. Tectonic setting of basic volcanic rock determined using trace element analyses. Earth and Planetary Sciences Letters, 19: 290-300.
Pearce, T. H., Gorman, B. E., Birkett, T. C., 1975. The $TiO_2 – K_2O – P_2O_5$ diagram a method of discriminating between oceanic and non – oceanic basalts", Earth and Planetary Sciences Letters, 24: 419-426.
Pearce, T. H., Gorman, B. E., Birkett, T. C., 1977. The relationship between major element geochemistry and tectonic environment of basic and intermediate volcanic rocks. Earth Planet Sciences Letters, 36: 121-132.
Pearce, J.A., Norry, M.J., 1979. Petrogenetic implications of Ti, Zr, Y, and Nb variations in volcanic rocks. Contributions to Mineralogy and Petrology, 69: 33-47.
Pearce, J.A., 1983. Role of sub-continental lithosphere in magma genesis at active continental margins. In: Hawkesworth, C.J., Norry, M.J. (Eds.). Continental basalts and mantle xenoliths Shiva: 230-249.
Pearce, J.A., Lippard, S.J., Roberts, S., 1984. Characteristics and tectonic significance of supra-subduction zone ophiolites. In: Kokelaar, B.P, Howells, M.F. (Eds.). Marginal Basin Geology: Volcanic and Associated Sedimentary and Tectonic Processes in Modern and Ancient Marginal Basins. Geological Society, London, Special Publication, 16:77-94.
Penrose Conference (participants), 1972. Penrose field conference on ophiohtes. Geotimes, 1: 24-25.
Ricou, L. E., 1971. Le croissant ophiolitique peri-arabe, un ceinture de nappes mises en place au Cretace superieur. *Review* of *Physical Geography* and *Dynamic Geology,* 13: 327-350.
Polat, A., Appel, P.W.U., Fryer, B.J., 2011. An overview of the geochemistry of Eoarchean to Mesoarchean ultramafic tomafic volcanic rocks, SW Greenland: implications for mantle depletion and petrogenetic processes at subduction zones in the early Earth. Gondwana Research, 20: 255–283.
Rolland, Y., Pecher, A., Picard, C., 2000. Middle Cretaceous back-arc formation and arc evolution along the Asian margin: the Shyok Suture Zone in northern Ladakh (NW Himalaya). Tectonophysics, 325: 145-173.
Ross, P.S., Bédard, J.H., 2009. Magmatic affinity of modern and ancient subalkaline volcanic rocks determined from trace element discriminant diagrams. Canadian Journal of Earth Sciences, 46(11): 823-839.
Sadeghi, Sh., Yassaghi, A., 2016. Spatial evolution of Zagros collision zone in Kurdistan, NW Iran: constraints on Arabia–Eurasia oblique convergence. Solid Earth, 7: 659–672.
Saccani, E., Allahyari, Kh., Beccaluva, L., Bianchini, G., 2013. Geochemistry and petrology of the Kermanshah ophiolites (Iran): Implication for the interaction between passive rifting, oceanic accretion, and OIB-type components in the Southern Neo-Tethys Ocean. Gondwana Research, 24: 392–411.
Saunders, A.D., Tarney, J., 1979. The geochemistry of basalts from a back- arc spreading center in the East Scotia arc. Geochemica et Cosmochemica Acta, 43: 555-572.
Saunders, A.D., Tarney, J., 1984. Geochemical characteristics of basaltic volcanism within back-are basins. In: Kokelaar, B. P., Howells M (Eds.). Marginal Basin Geology. Geological Society of London Special Publication, 16: 59-76.
Saunders, A.D., Tarney, J., 1991. Back-arc basins. In: Floyd, P (Ed.) Ocean Basalts. Blackie, London: 219-263.
Serri, M., 1981. Petrochemistry of ophiolite gabbroic complex: A key for classification of ophiolites into low-Ti and high Ti types, Earth and Planetary Science. Letters, 52: 203-212.
Shafahii Moghadam, H., Stern, R. J., 2011. Late Cretaceouse fore arc ophiolites of Iran, Island Arc, 20: 1-4.
Shafahii Moghadam, H., Khedr, M. Z., Chiaradia, M., Stern, R. J., Bakhshizad, F., Arai, S., Ottley, C. J., Tamura, A., 2014. Supra-subduction zone magmatism of the Neyriz ophiolite, Iran: constraints from geochemistry and Sr-Nd-Pb isotopes, International Geology Review, 56:11: 1395-1412.

Shahidi, M., Nazari, H., Geological map of Harsin, 1/100.000 scale, Geological survey of Iran, Tehran, 1997**.**

Shervais, J.W., 1982. Ti-V plots and the petrogenesis of modern and ophiolitic lavas. Earth and Planetary Science Letters, 59: 101-118.

Schiffman, P., Fridleifsson, G.O., 1991. The smectite-chlorite transition in drill hole Nj-15, NesjaveUir geothermal field, Iceland: XRD, BSE and electron microprobe investigations. Journal of Metamorphic Geology, 9: 679-696.

Stocklin, J., 1974. Possible ancient continental margin in Iran. In: Burke, C.A., Drake, C.L. (Eds.). The Geology of Continental Margins. Springer, New York: 873-887.

Sun, S. S., Mc Donough, W. F., 1989. Chemical and isotopic systematic of oceanic basalts: implications for mantle composition and processes. In Sunders A. D., Norry M (Eds.) Magmatism in oceanic Basins", Geological Society of London Special publication, 42: 313-345.

Takin, M., 1972. Iranian geology and continental drift in the Middle East. Nature, 235: 147-150.

Winchester, J.A., Floyd, P.A., 1977, Geochemical discrimination of different magma series and their differentiation products using immobile elements. Chemical Geology, 20: 325-343.

Whitechurch, H., Omrani, J., Agard, P., Humbert, F., Montigny, R., Jolivet, L., 2013. Evidence for Paleocene–Eocene evolution of the foot of the Eurasian margin (Kermanshah ophiolite, SW Iran) from back-arc to arc: Implications for regional geodynamics and obduction. Lithos, 182-183: 11-32.

Wilson, M., 1996. Igneous petrogenesis" Unwin Hyman London, 450 p.

Yumul, Jr., G.P., 1993. Supra-subduction zone Ophiolites – promising exploration targets? Evidence from the Zambales ophiolite complex, Luzon, Philippines. Resource Geology Special Issue, 15: 157-170.

Yumul, Jr., G.P., 1996. Review of the Geochemistry of mid-ocean ridge and supra-subduction zone Ophiolites: Comparison and discussion. Journal of Geological Society of Philippines, LI (1/2): 3-36.

Yumul, Jr., G.P., Balce, G.R., 1994. Supra-subduction zone Ophiolites as favorable hosts for chromite, platinum and massive sulfides. Journal of Asian Earth Sciences, 10: 65-79.